Cyclic Re-Ignition Phenomena in Constant Volume Combustors

C. Runnoo[1]*, Q. Michalski[2], B. Boust[1] and M. Bellenoue[1]

1: PPrime Institute, CNRS, ISAE-ENSMA, Poitiers University, France
2: School of Aerospace, Mechanical and Manufacturing, RMIT University, Australia

* Correspondent author: naina.runnoo@ensma.fr

Abstract

This work investigates cycle hysteresis issues associated with operating a constant volume combustor concept applied to a pistonless gas turbine. Experimental tests are carried out on a lab-scale combustion vessel (CV2) operated for finite cyclic operation. This facility features the turbulent combustion of air and fuel direct-injection, with a controlled overall equivalence ratio. Operating conditions are set to reach either spark-ignited flame propagation or re-ignition induced by residual burned gases. Chemiluminescence recordings of OH* and CH* were performed to shed light onto the phenomenology of re-ignition processes. Re-ignition events form over two cycles whereupon the first spark-ignited cycle leads to a slow flame propagating during the exhaust phase. At the start of the following cycle, air injection is associated with an increase in chemiluminescence followed up by quick re-ignition at fuel injection timing.

Keyword: *constant volume combustion, auto-ignition, radical intensity, residual burned gas*

1. Introduction

Alternative combustion cycles such as Pressure-Gain Combustion (PGC) are promising methods for reducing fuel consumption and emissions in aircraft engines [1]. Constant Volume Combustion (CVC) is a conventional PGC technology widely used in piston engines. Pistonless CVC systems are gaining attention, in such chambers, aerodynamic-driven mixing and scavenging replace mechanical pistons. In such chambers, large-scale aerodynamics persist much longer, hindering ignition and leading to uncontrolled re-ignition (RI) under low-scavenging conditions [2][3][4][5]. Additionally, achieving the necessary power density for flight requires high cycle frequencies, limiting mixing time and turbulence decay, mandating more complex spark-ignition strategies [6]. In these regimes, re-ignition could then become advantageous and, if controlled, be used as an ignition mechanism. However, the exact conditions in which RI occurs are not well understood. Previous studies with propane-air mixture on the same device suggested that the ignition mechanism strongly depends on the mixing between hot exhaust gases and lean fresh mixtures, reported thermal imaging, but did not investigate any residual chemical activity in the residual burnt gases (RBG) [7]. The re-ignition mechanism is believed to be akin to pre-burners developed for CVC applications. Previous investigations [8][9][10] where high-temperature, radical-rich jets replace spark plugs some including CVC [8][11][12] relied on OH* chemiluminescence to characterize the ignition process. In this study, the re-ignition phenomena are characterized using OH* and CH*chemiluminescence to discriminate whether the RI mechanism is purely thermal or if residual chemical activity persisting in the RBG could have an influence. Using liquid n-heptane, this study identifies a hybrid operational point where re-ignition occurs consistently after the exhaust phase of a spark-ignited cycle.

2. Experimental setup

The experimental setup in this study simulates the cyclic conditions of CVC and mass flow rates typical of expected combustors [7]. Its modular design allows various geometrical configurations as outlined in multiple patents [13][14]. A single chamber is studied to understand its internal physics accounting for potential integration effects. The chamber is a rectangular parallelepiped, machined from stainless steel (17-4 PH), with a maximum internal volume of 150×50×50 mm (Fig. 1 (i)). The combustion chamber features wide, shoulder-mounted optical access made of 7980 KrF UV silica, providing full access to the internal cuboidal volume and enabling recordings of chemiluminescence emitted by excited chemical radicals during the combustion phase. The main components, therefore, include the combustion chamber as well as an intake and exhaust systems, operating over 10 to 20 cycles, allowing precise measurement of injected air mass and control of exhaust back pressure. Two fast solenoid valves, COAX MK10, control the air intake and exhaust. The constant volume

part is formed by the sum of the chamber's internal volume (0.125/0.250/0.375 L) increased by the respective internal volumes of the valves, flanges, and tubes connecting to the chamber.

A spark plug flush mounted to the wall is used to ignite the mixture and start the combustion. Before starting of the combustion, the initial conditions of pressure and temperature are fixed. The pressure is monitored using a piezoresistive sensor (Kistler 4049B), which records the combustion pressure rise and enables the dynamic acquisition of up to 2 MPa. Proportional-integral-derivative (PID) controllers regulate the temperature of the air tank (423 K) and combustion chamber (403 K). The CVC cycle consists of sequential intake, combustion and exhaust phases. A typical pressure evolution in spark ignition (SI) case (ignition delay of 25 ms) is presented Fig. 1(ii).

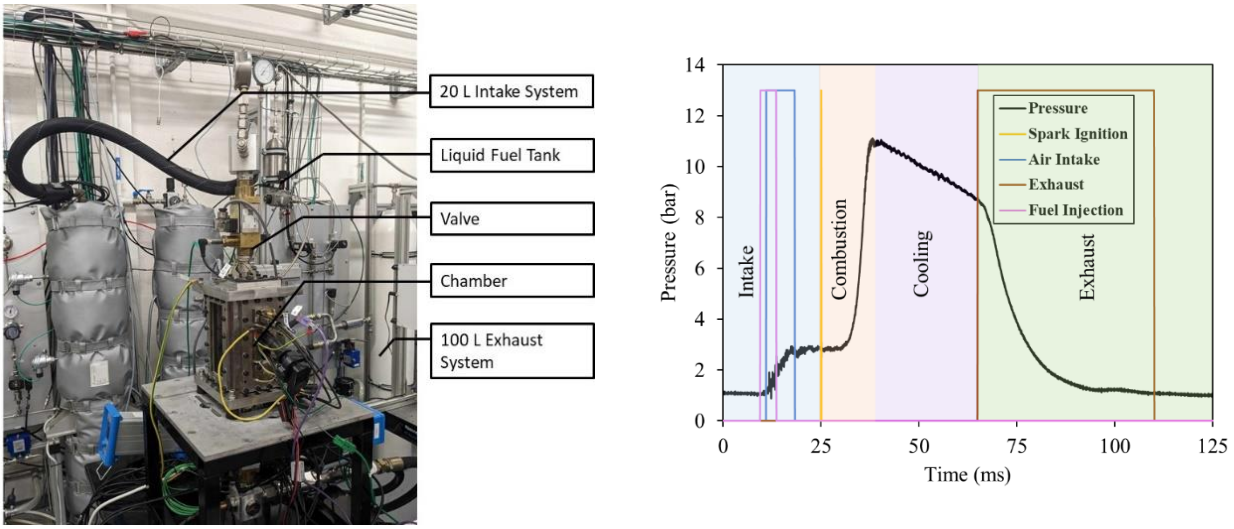

(i) Experimental set up (ii) Typical pressure evolution of one SI cycle

Fig. 1 Experimental set up and typical pressure evolution of one spark ignition cycle

2.1 CV2 operating methodology

During the intake phase, compressed air at 1 MPa stagnation pressure, is introduced inside the combustion chamber through the intake valve yielding mass flow rates in the order of 80 g/s at peak opening. Simultaneously a gasoline injector, Bosch HDEV, flush mounted to the wall delivers liquid n-heptane, pressurized at 10 MPa with nitrogen, directly into the chamber. The mass flow rate of n-heptane is about 8.4 g/s. Liquid n-heptane was chosen for its high cetane number (approximately 56) and low auto-ignition temperature (204 °C) to further promote auto-ignition. For the tests, pressure drop in the air tank is continuously measured to determine the overall injected equivalence ratio of the fresh reactants. Fuel pressure remains constant during the test [7]. Fuel mass was determined preliminary by injector calibration. Spark ignition cycles are used as a first step to identify stable operating points offering a repeatable baseline for analysis, before carrying RI tests. The current methodology aims to establish operating points that facilitate this phenomenon. RI events are influenced by the transient mixing between RBG, the directly injected fuel and the freshly admitted air. Therefore, parameters such as exhaust pressure and ignition timing were varied to promote its occurrence. Sensitivity tests on ignition timing were conducted to determine occurrence of successful re-ignition sequence keeping stoichiometric mixture for exhaust pressure of 1 or 2 bar (Fig. 4).

2.2 Chemiluminescence imaging

Chemiluminescence emitted by chemical radicals in flames can be employed both quantitatively and qualitatively as a diagnostic tool for combustion in internal combustion engines, burners, turbines, and other combustion systems [15]. A high-speed camera (Photron SA5) records the chemiluminescence at a framerate of 1000 fps and a resolution of 640×1024 pixels. OH* (306 nm) and CH* (430 nm) filters are sequentially placed on the camera lens. Simultaneously, a second high-speed color camera (Phantom V310) records broadband chemiluminescence to distinguish between rich and lean cycles through the presence of broadband soot radiation. An overall OH* chemiluminescence level is defined based on the sum of total pixel intensity

over all pixel in each image and is used to detect the onset of combustion. The OH* chemiluminescence identifies high-temperature reaction zones and, in particular, could be present in the RBG. These RBG, if at elevated temperatures, still contain significant fractions of OH*. Thus, OH* can be used to track not only the active combustion zone but also regions with high residual heat from burnt gases. In previous works, OH* chemiluminescence was used as an indicator of heat release during the combustion process, with its peak emission aligning with the point of maximum heat release within the combustion chamber [15]. The CH* chemiluminescence tracks the flame front. In premixed flames CH forms temporarily within the flame front thus CH* emission is more focused on the initial stages of combustion and flame propagation where chemical reactions dominate.

3. Results and discussion

3.1 Influence of delayed ignition timing on the stability of re-ignition

In this section, a first set of 14 tests was carried out at stoichiometry, with at an air intake valve opening duration of 11 ms and fuel injection duration of 6 ms. The cycle frequency is kept at 8 Hz, hence a period of 125 ms, and the sequence contains 20 cycles. The exhaust valve timing was set to 55 ms and the exhaust valve duration to 45 ms with the exhaust pressure of 1 bar. Ignition timings were delayed from 30 ms to 100 ms to observe the influence of delayed ignition timing on re-ignition. The temporal pressure evolution for different ignition time (t_{ign}) is shown in Fig. 2.

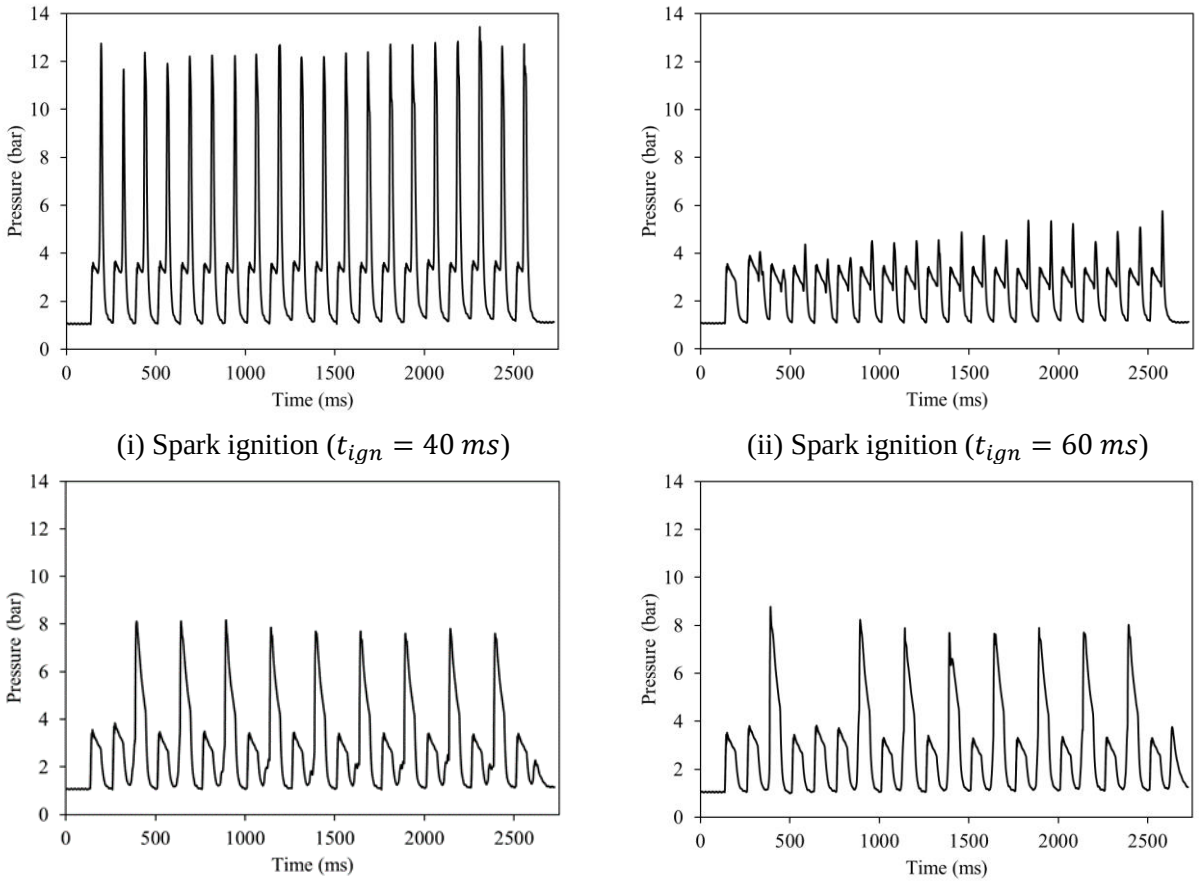

(i) Spark ignition ($t_{ign} = 40\ ms$) (ii) Spark ignition ($t_{ign} = 60\ ms$)

(iii) Re-ignition ($t_{ign} = 85\ ms$) (iv) Re-ignition ($t_{ign} = 100\ ms$)

Fig. 2 Temporal pressure evolution for different delayed ignition timing

Delaying the ignition timing strongly affects cycle stability (see Fig. 2). At a t_{ign} of 40 ms, consistent spark-igntion cycles were obtained, indicating optimal combustion behavior with high pressure gain and little to no cycle hysteresis. When t_{ign} is increased to 60 ms, the combustion process occurs mainly during the exhaust phase and the overall pressure gain reaches its minimum. At a t_{ign} of 85 ms, reproducible patterns of re-

ignition were observed. Further increasing the t_{ign} to 100 ms, still yields re-ignition but cycles lacked consistency and reproducibility.

A zoomed-in analysis with a clear breakdown of each phase for each cycle type, spark ignition and re-ignited, is then performed (Fig. 3).

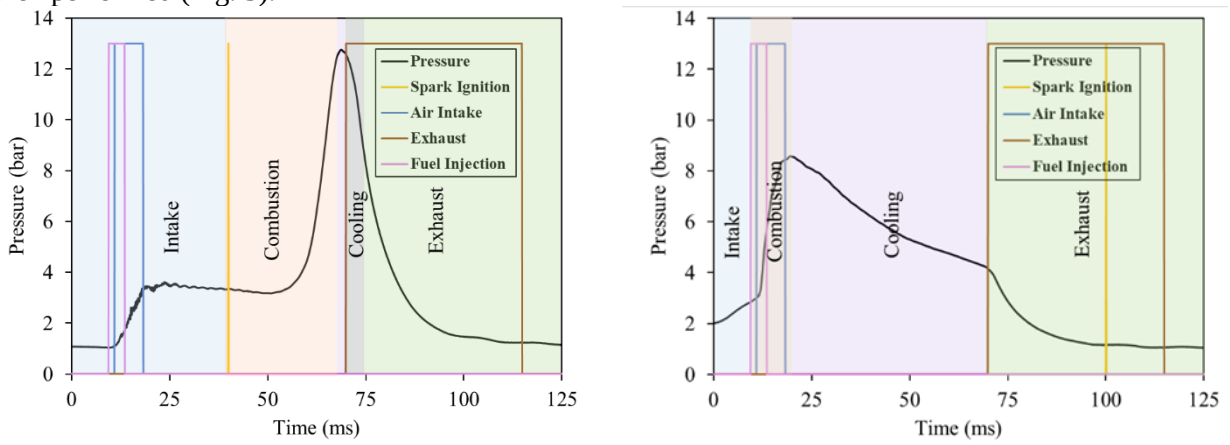

(i) Spark-ignition cycle (ii) Re-ignition cycle

Fig. 3 Spark-ignition cycle vs Re-ignition cycle

In a spark-ignited cycle (Fig. 3(i)), air and fuel are mixed during the intake phase. Spark-ignition initiates the constant volume combustion, followed by the exhaust phase. The exhaust timing was optimized to reduce any isochoric cooling phase. In contrast, in a re-ignited cycle (Fig. 3(ii)), combustion occurs within the intake phase, followed by cooling and exhaust phase prior to the spark ignition timing.

A statistical analysis of re-ignition sequences (RIS) is performed, varying the ignition delay and the back pressure. A RIS is defined as sequences where every other cycle re-ignites, excluding any initial misfires. A RIS success rate p_{RIS} can then be calculated, while omitting the first misfired cycles (hence, number of cycles of 18 instead of 20), to avoid possible incomplete RIS:

$$p_{RIS} = \frac{2R}{R+S} \tag{1}$$

Where R = number of re-ignited cycles and S = number of spark-ignited cycles. Ignition timings of 30 to 60 ms showed $p_{RIS} = 0\%$, 65 and 70 ms showed p_{RIS} = 22%, and up to 100% at 85 ms. RIS decreases slightly to 94% at 90 and 100 ms for a back pressure of 1 bar as shown in Fig. 4. Increasing the backpressure overall, increases p_{RIS} at similar ignition timings suggesting higher amount of RBG does promote re-ignition.

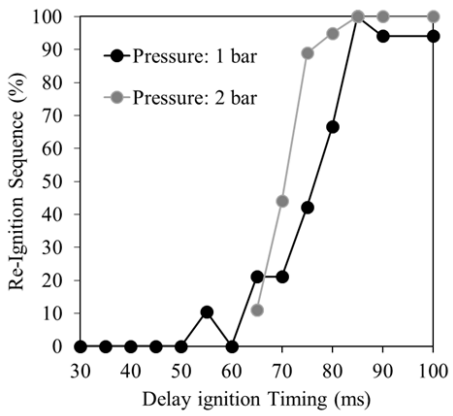

Fig. 4 Percentage of re-ignition sequence obtained at different delayed timing

3.2 Analysis of radical contributions to re-ignition phenomena

To further investigate re-ignition, a case with 100% RIS was examined at an increased frequency of 12.5 Hz (hence a period of 80 ms) over 10 cycles, with an exhaust pressure of 2 bar and a leaner equivalence ratio of 0.8 (air intake duration of 11 ms and fuel injection duration of 5 ms). The exhaust valve timing was set to 30 ms and the exhaust valve duration to 30 ms. The ignition timing was set to 55 ms. To analyze the phenomenology of re-ignition, OH* and CH* emissions are considered here. The quantitative metric used is the total pixel intensity obtained by summing all pixel values on each image. The OH* tests were conducted first, followed by the CH* tests under identical conditions. Since separate tests are performed for both OH* and CH* measurements, pressure traces were carefully analyzed to select the optimal cycles to compare OH* with CH* levels (see Fig. 5). The integration time is tuned to capture the low luminosity levels of the spark-ignited flames, the camera thus saturates during the re-ignition phase of the following cycle. The normalized pressure and normalized pixel intensity of OH* and CH* were represented. The time evolution of the total pixel intensity of OH* and CH* of a referenced spark-ignited cycle and re-ignition cycle is plotted on Fig. 5(i) and respectively on Fig. 5(ii).

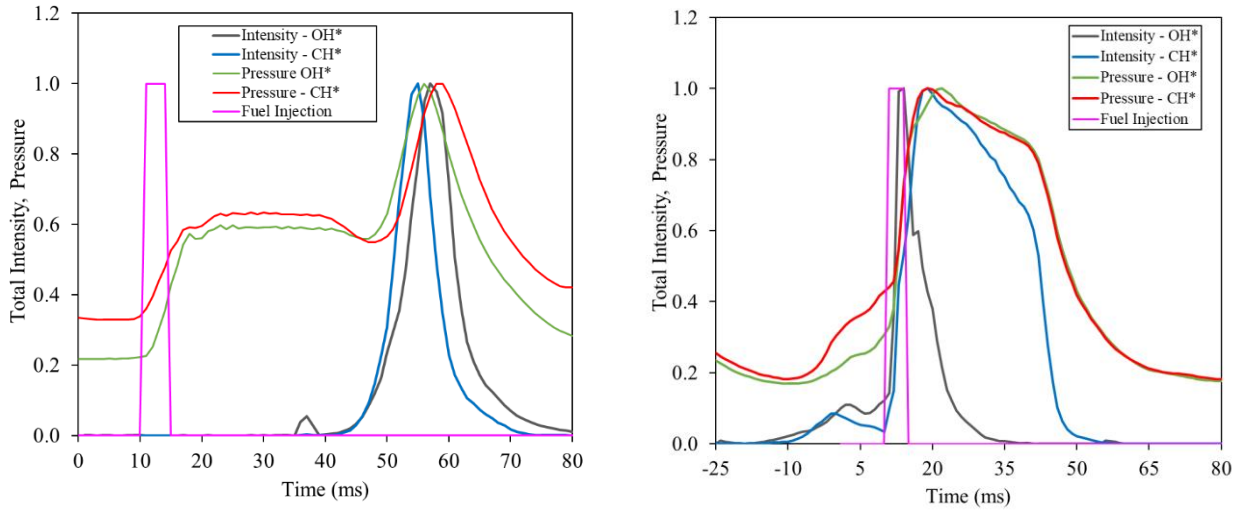

(i) Spark ignition cycle (ii) Re-ignition cycle

Fig. 5 Time evolution of total pixel intensity of OH* and CH*

For a referenced case of a spark-ignited cycle Fig. 5(i), OH* and CH* behave similarly. The heat release is on the partially pre-mixed flame as can be seen in Fig. 6. Fig. 5(ii) consists of two cycles: a previously spark-ignited cycle (from – 25 ms to 0 ms) and the re-ignited cycle. In the initial SI cycle, CH* rises sharply indicating the formation of the flame front and early-stage chemical reactions. OH* rises more gradually, closer to its respective peak pressure. OH* emission is associated with high-temperature zones in the flame and post-flame regions. The combustion chamber eventually only contains RBG which includes hot combustion products and reactive radicals following the initial combustion (SI) cycle. At the end of the SI combustion, OH* chemiluminescence remains observable, suggesting the RBG are still chemically active. These gases, consisting of partially oxidized combustion products and reactive species, persist in the chamber as the next cycle starts again. At around 9 ms, fuel is injected into the chamber, leading to the formation of a new fuel-air mixture. Unlike in the SI cycle, the fresh reactants mix with high temperature RBG from the previous (SI) cycle. The presence of OH and CH radicals, attested by non-zero levels of chemiluminescence, facilitates the re-ignition of the fresh fuel-air mixture without requiring an additional spark. The re-ignition begins when the newly injected fuel interacts with the RBG. This is evidenced by an increase in CH* chemiluminescence, which indicates the establishment of a flame front in the re-ignited cycle. The subsequent rise in OH* chemiluminescence reflects the development of high-temperature zones and the progression into the main heat release phase of combustion. The pressure within the chamber also rises following fuel injection and re-ignition, simultaneously to the peaks in CH* and OH*.

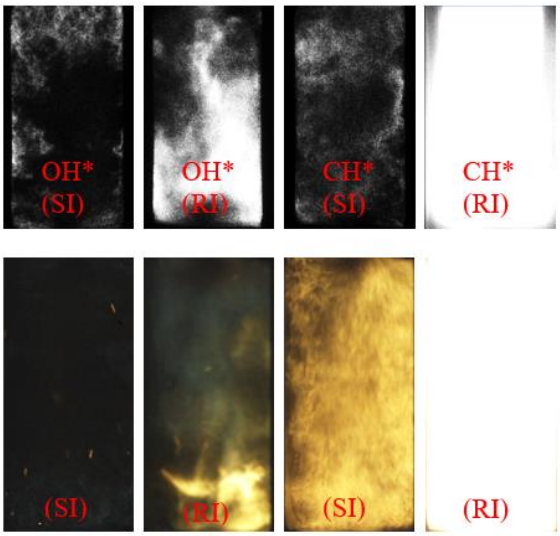

Fig. 6 Comparison of radical emission at maximum pressure obtained from the black and white camera and the colored camera

Analyzing further Fig. 6, it can be observed that for the re-ignition cycle, the OH* and CH* emissions behave differently. However, both OH* and CH* are more intense in a re-ignition cycle compared to a spark-ignited cycle. In the re-ignition cycle, the OH* is simultaneous to the heat release while CH* persists for a longer duration much unlike the SI cycle. This extended CH* emission is attributed to rich diffusive combustion, absent in the spark ignited cycle. Since mixing time is limited in RI cycles, extremely rich pockets are formed and diffusive combustion persists after the main heat release.

4. Conclusion

This research investigates residual burnt gases as an alternative ignition method for Constant Volume Combustion. Delayed spark ignition is identified as the main parameter driving cycle stability and leading to consistent re-ignition events. Increasing the exhaust pressure increases the amount of residual burnt gases leading to increase in re-ignition probability. Re-ignition events, observed over two cycles through chemiluminescence, show that the initial cycle is spark-ignited, leading to a slow flame during the exhaust phase. Following the spark-ignited cycle, the chamber retains RBG containing OH* and CH* radicals. At the onset of the second cycle, the mixing of fuel and air with the still-burning gases results in the re-ignition of the mixture. The OH* signal peaking shortly after fuel injection in the re-ignition stage, indicated high-temperature regions during the quick combustion phase. Moreover, despite an overall lean injected equivalence ratio, the combustion occurs in rich pockets due to poor mixing. Sustained CH* emission past the peak pressure confirms a slower diffusion flame also occurs following the main heat release combustion event.

Acknowledgements and Funding

The authors are grateful to the Région Nouvelle Aquitaine for the financial support of fast optical diagnostics; Emilien Brodu, Alain Claverie and Rédouane Kari for the technical support. The paper is based upon work supported by the European Union's Horizon 2020 INSPIRE program under the Marie Skłodowska-Curie grant agreement No 956803.

References

[1] M. Bellenoue *et al.*, "New Combustion Concepts to Enhance the Thermodynamic Efficiency of Propulsion Engines" (2016).

[2] Q. Michalski, B. Boust, and M. Bellenoue, "Toward a cyclic self-ignited constant-volume combustion for airbreathing propulsion applications," *Joint Propulsion Conference, American Institute of Aeronautics and Astronautics Inc, AIAA* (2018).

[3] "Finno Exergy's PGC Technology: a novel solution for efficiency improvement and fuel flexibility in gas turbines," (2023).C

[4] B. Boust, Q. Michalski, and M. Bellenoue, "Experimental investigation of ignition and combustion processes in a constant-volume combustion chamber for air-breathing propulsion," in *52nd AIAA/SAE/ASEE Joint Propulsion Conference, American Institute of Aeronautics and Astronautics Inc, AIAA*, (2016).

[5] G. Exilard, Y. Mery, and S. Richard, "Large Eddy Simulation of Constant Volume Combustion in an aeronautical engine."

[6] Q. Michalski, B. Boust, and M. Bellenoue, "Experimental Investigation of Ignition Stability in a Cyclic Constant-Volume Combustion Chamber Featuring Relevant Conditions for Air-Breathing Propulsion," Flow Turbulent Combustion, Vol. 102, No. 2, (2019), pp. 279–298.

[7] Q. Michalski, "Etude expérimentale de la combustion à volume constant pour la propulsion aérobie : influence de l'aérodynamique et de la dilution sur l'allumage et la combustion," École Nationale Superieure De Mecanique et d'Aerotechnique, (2019).

[8] S. Biswas, "Physics of Turbulent Jet Ignition Mechanisms and Dynamics of Ultra-lean Combustion."

[9] Q. Tang et al., "Optical diagnostics on the pre-chamber jet and main chamber ignition in the active pre-chamber combustion (PCC)," *Combustion Flame*, Vol. 228, (2021) pp. 218–235.

[10] P. M. Allison, M. de Oliveira, A. Giusti, and E. Mastorakos, "Pre-chamber ignition mechanism: Experiments and simulations on turbulent jet flame structure," *Fuel*, Vol. 230, (2018), pp. 274–281.

[11] S. Biswas, S. Tanvir, H. Wang, and L. Qiao, "On ignition mechanisms of premixed CH4/air and H2/air using a hot turbulent jet generated by pre-chamber combustion," *Applied Thermal Engineering*, Vol. 106, (2016) pp. 925–937.

[12] S. Biswas and L. Qiao, "Ignition of ultra-lean premixed H2/air using multiple hot turbulent jets generated by pre-chamber combustion," *Applied Thermal Engineering*, Vol. 132, (2018), pp. 102–114

[13] M. Leyko, P. Moissy-Cramayel, and J. Metge, "Constant-volume combustion system comprising a rotating closure element with segmented apertures", (2018).

[14] M. Leyko, "Constant-volume combustion module for a turbine engine, comprising communication-based ignition."

[15] F. V. Tinaut, M. Reyes, B. Giménez, and J. V. Pastor, "Measurements of OH* and CH* chemiluminescence in premixed flames in a constant volume combustion bomb under autoignition conditions," *Energy and Fuels*, Vol. 25, No. 1, (2011) pp. 119–129.